Combined digestion and bleaching of New Zealand flax /harakeke fibre and its effects on the mechanical, thermal, and dynamic mechanical properties of poly(lactic) acid matrix composites

John O. Akindoyo, Kim Pickering, Mohammad Dalour Beg and Michael Mucalo

School of Science and Engineering, The University of Waikato, Private Bag 3105, Hamilton, New Zealand

Correspondence: John Olabode Akindoyo (blessedbode@ymail.com: +64274168550)

Abstract

In this study, New Zealand flax (harakeke) fibre was initially modified through digestion in an alkali solution followed by bleaching with hydrogen peroxide and sodium silicate with the aim of improving thermal and mechanical performance of its composites, through increased interfacial bonding. X-ray diffraction analysis (XRD), Fourier transform infrared spectroscopy and lignin analysis showed that the combination of bleaching and alkali treatment resulted in a higher cellulose content than digestion alone. Fibre inclusion was found to increase the crystallinity of PLA, likely due to heterogeneous nucleation on the treated fibres, which in turn helped to improve the composite strength. The highest tensile strength, tensile modulus and thermal stability were achieved with the bleached fibre which is believed to be due to better fibre distribution and stronger interfacial interaction. This was supported by the adhesion factor and effectiveness coefficient calculated using the data obtained from dynamic mechanical analysis.

Keywords: A. Polymer matrix composites (PMCs); B. Mechanical properties, Adhesion; E. Injection moulding

1. Introduction

In recent years, there have been increasing efforts on developing environmentally friendly materials through a synergy between the principles of green chemistry, sustainability, and eco-efficiency [1, 2]. This is aimed at reducing the excessive dependence on fossil fuel and petroleum-based products [3, 4]. In this regard, biodegradable or renewable polymer-based composites are examples of materials that can be used. This is because polymers are very versatile, can be used in different applications, and can be modified to meet specific purposes [5].

Poly (lactic) acid (PLA) is one polymer that has been widely investigated as a substitute for non-degradable high environmental impact polymers, as detailed in different research and review articles [6-9]. The strength and stiffness of PLA is sufficient for different packaging, medical, and other non-structural applications where high load bearing is not a priority. In addition, the inherent biodegradability and processability of PLA mean that its properties can be tuned to obtain whatever desired performance that is fit for purpose [5, 10]. Hence, PLA has been combined with natural fibres to produce environmentally benign composites with improved mechanical strength. This is partly associated with the salient properties of natural fibres such as low cost, renewability, biodegradability, recyclability, low density, high flexural strength, high modulus, and non-abrasiveness [11, 12]. Studies have shown that good interfacial shear strength (IFSS) in natural fibre reinforced PLA can significantly affect the composite strength. For example, the work by Setswalo et al. on mukwa/PLA composites demonstrated higher flexural properties with improved IFSS, obtained through fibre treatment

[13]. Similarly, Tarrés et al. demonstrated that a weak interphase can result in reduced tensile strength [14]. In a different study, a hybrid natural fibre (coir/pineapple leaf fibres) system was used to reinforce PLA. It was found that the untreated hybrid biocomposite returned a higher damping factor and lower strength, attributed to weak interphase [15]. Generally, most studies on natural fibre reinforced PLA composites are focussed on improving interfacial interaction between PLA and the fibres through chemical bonding, or interfacial adhesion [6, 7, 9, 11]. However, too much fibre can lead to insufficient wetting by the matrix which in turn results in poor interface between the fibre and the matrix leading to reduced strength. In relation to that, there have been several articles on the effect of fibre content on the properties of PLA. For example, Abdallah et al. investigated the effect of varying fibre content (0-40 wt.%) on the mechanical and thermal insulation properties of date palm fibre reinforced PLA [16], and found that the tensile strength was remarkably high up to 20 wt.% fibre content. Serizawa et al. also reported 20 wt.% as the optimum fibre content in kenaf fibre reinforced PLA composites [17]. Similarly, Komal et al. reported 20 wt.% as the optimum fibre content after preparing 10-30 wt.% banana fibre reinforced PLA composites [18].

Generally, the conventional natural fibres used as reinforcement in PLA composites include oil palm empty fruit bunch, sisal, hemp, flax, coir, bagasse, banana, and jute [10, 19, 20]. In the past decade, there has been increasing interest in the use of fibres extracted from the leaves of *Phormium tenax* commonly called New Zealand flax (harakeke), as reinforcement in polymer composites. Harakeke is indigenous to New Zealand and the Norfolk Island, and it is a significant resource in Māori culture for making woven mats and containers. In terms of morphology and anatomy, harakeke leaves are clumped together in groups and tend to be folded at their stem. The leaves can grow to a length of about 3 m, and extend to about 50-120 mm in width [21]. The structure of harakeke leaf is one that is typical of monocotyledons. There is a spiral overlap at the base of the fibre, which lies parallel to bundles of sclerenchyma fibres. These sclerenchyma fibres are bonded together by lignin and hemicellulose, but the bonds can be broken by dissolution in an alkali solution, or in boiling water [22]. Fibres obtained from harakeke leaves were historically used for producing cloaks, ropes, and for making baskets and fishing nets [23]. These uses suggest that harakeke leaves could offer good reinforcement properties. Therefore, some studies have explored the possibility of combining harakeke fibre with different polymers [22, 24, 25]. However, reports on harakeke fibre as reinforcement in injection moulded PLA for producing composites suitable for structural applications are few in the materials science literature. It is well known that the notable determinants of the suitability of composites for structural applications are the reinforcing ability of the fibre, compositional balance, and the extent of interfacial adhesion between the fibre and the matrix. Therefore, these are given prime consideration in this article.

Interfacial adhesion in natural fibre composites is commonly improved through chemical modification of the fibre, with most studies focussing on facilitating surface roughness through alkali treatment [26, 27]. This has reportedly

produced significant improvement in tensile strength and tensile modulus due to removal of components that can lead to weak interface from the fibre. In addition, alkali treatment helps to expose the cellulose hydroxyl groups of the fibre for bonding with the matrix which in turn facilitates mechanical interlocking between the fibre and the matrix [28]. The use of coupling agents, or the combination of other chemical techniques with alkali treatment can also help to improve interfacial adhesion in natural fibre reinforced composites. Peroxide treatment is one of such chemical treatments that can be combined with alkali treatment to improve the chemical bonding between natural fibres and polymer matrices [10]. The mechanism of peroxide treatment suggests that it can generate good mechanical and thermal resilience in natural fibres, as well as facilitate strong chemical bonding and thermal resilience in fibre reinforced composites by acting as a fibre modifier and as a coupling agent. Despite the potential of peroxide treatment to produce significant improvements in composite properties, it is less commonly reported in the literature and so, it is worthy of deeper investigation. Therefore, the aim of this study is to investigate the effect of combined digestion and peroxide treatments on harakeke fibre, and its reinforcing properties in PLA composites as it relates to its suitability for structural applications.

2. Materials and methods

2.1. Materials

The harakeke fibre used as reinforcing filler in this study was kindly supplied by Templeton Flax Milling Heritage Trust, New Zealand. The polymer matrix used is Ingeo™ Biopolymer 3052D poly (lactic acid) (PLA) from NatureWorks. This PLA is an injection molding grade with a specific gravity of 1.24 and melt flow rate (MFR) of 14 g/10 min (210 °C, 2.16 kg). Sodium hydroxide bulk grade solid pellets, sodium sulfite powder, and hydrogen peroxide (30%) were purchased from Sigma-Aldrich and used without further purification. In addition, extra pure sodium silicate (Na_2SiO_3) solution, and sulfuric acid (96%) were procured from Merck Millipore.

2.2. Methods

2.2.1. Preparation and treatment of harakeke fibre

The harakeke fibre, as received, had a length of about 1-1.5 m. After drying, the fibre was cut into 2-3 cm pieces using a guillotine. Weighed amounts of the chopped fibre were placed in stainless steel canisters and digested using a solution of 5 wt.% NaOH and 2 wt.% Na_2SO_3 in a lab-scale pulp digester. The ratio of fibre to solution was kept at 1:8, and a programmed controller was used to run the digester over a 4-step cycle which included a treatment temperature set at 160 ºC and a holding time of 2 h. After digestion, the treated fibre was thoroughly washed under a continuous water flow until the pH of the wash water was measured as neutral at pH 7. The washed and treated fibres were then dried in a laboratory oven set at 80 ºC for 48 h after which the dried fibres were stored in a sealed plastic bag until used for further analysis and for composite fabrication.

Bleaching of harakeke was performed using a solution of H_2O_2 and Na_2SiO_3. For this process, 45 g of digested fibre was placed in 3 L of Milli-Q distilled water. The water was first heated to 70 ºC, and the fibre was introduced under continuous stirring for about 15 min after which 75 mL of Na_2SiO_3 (2.5% by volume) was added. After 5 min, 150 mL of H_2O_2 (5% by volume) was added and the bleaching process was allowed to continue under rigorous stirring for an additional 10 min. After completion of the bleaching process, the bleached fibre was washed under a water flow until the waste wash water showed a neutral pH. Then the fibre was dried at 80 ºC for 48 h and stored in a sealed plastic bag until used for further analysis and composite production.

2.2.2. Determination of lignin and carbohydrate content in harakeke fibre

The amount of lignin in the raw, digested, and bleached harakeke fibre was determined according to the Round Robin method for determination of Klason lignin as detailed in the Technical Association of the Pulp and Paper Industry (TAPPI) T 222 om-02 test methods. Briefly, weighed amounts of the dry fibre were digested in a 72% (w/w) H_2SO_4 solution inside a test tube, with the mixture being stirred with a glass rod until dissolution began. The mixture containing test tube was placed in a water bath for 1 h at 30 °C with occasional stirring. The mixture was further diluted to ~ 3% (w/w) H_2SO_4 in a beaker using distilled water, and placed in an autoclave set at 121 °C. After 1 h, the beaker was cooled to 80 °C and the mixture was filtered using a vacuum filter to separate the insoluble matter. The acid insoluble residue (AIR) was subsequently allowed to dry overnight at 105 °C and the dry weight of acid insoluble residue (viz., Klason lignin) was calculated using equation 1 as follows:

$$Acid\ insoluble\ residue\ (AIR) = \frac{m}{M}\ x\ 1000 \qquad (1)$$

where, m is the dry weight of residue after acid hydrolysis, in g and M is the oven-dry weight of sample (100% dry matter) before acid hydrolysis, in g. The filtrate from the Klason lignin determination test was used to determine the acid soluble lignin, and the carbohydrate content of the samples. The carbohydrate (cellulose and hemicellulose) content was determined following a method described in literature for wood sugar analysis by anion chromatography [29].

2.2.3. Production of PLA/harakeke composites

Composites were produced from PLA and harakeke fibre using digested and bleached fibres at different fibre content (0-30 wt.%). The composite components were mixed and compounded using a twin screw extruder (Labtech LTE-20-44). Prior to extrusion, the dried treated fibres were sheared using a Sunbeam Multigrinder with blunt blades. Shearing was performed at a high rotational speed to defibrate the fibre. After this, the fibres were dried overnight in a conventional oven set at 105 °C. For the PLA granules, drying to moisture content < 0.1% was carried out using a vacuum oven set at 60 °C for 2 h. Then, extrusion was performed using a temperature profile in the range of 165-175 °C, with the feeding and die zones kept at 120 °C and 175 °C, respectively. After extrusion, the extruded materials were granulated

using a Moretto GR knife mill plastic granulator with an inserted sieve to obtain granules of about 3 mm in length. After drying the granules to a moisture content < 0.1% by weight, test samples were prepared using an injection moulding machine (BOY 35A). The injection profile used for test sample preparation includes a feeding zone temperature of 150 °C, a compression zone temperature of 165-185 °C, a metering zone temperature of 190 °C, a nozzle temperature of 185 °C, a mould temperature of 35 °C, injection time of 0.5 s and cooling time of 30 s. For easy identification, the different composite batches produced were given code names, with values 10, 20 or 30 indicating the wt.% fibre content while DF or BF represents digested fibre or bleached fibre, respectively. For example, "PLA represents the neat PLA matrix while "PLA+20 BF" represents the composite containing 20 wt.% bleached fibre.

2.2.4. Fourier transform infrared (FTIR) spectroscopy

The functional groups on the raw harakeke fibre, and changes in the FTIR spectra of digested and bleached harakeke fibre were analysed with a Perkin Elmer® Spectrum 100 FTIR spectrometer. Spectral analysis of the PLA was performed and compared with similar IR analyses of the PLA/harakeke composites. The FTIR data were recorded over a wavelength range of 4000 - 400 cm^{-1} using the standard KBr pellet technique.

2.2.5. Scanning electron microscopy (SEM)

Surfaces of the raw, digested, and bleached harakeke fibre were observed on a Hitachi Regulus SU8230 field emission scanning electron microscope. Likewise, the fractured surfaces of PLA and PLA/harakeke composites after tensile testing were examined. Prior to SEM observation, the samples were dried and mounted on aluminium stubs using double sided carbon tape. The mounted samples were subsequently sputter coated with a 5 nm layer of platinum in a Quorum Q150V sputtering equipment to make them conductive.

2.2.6. X- ray diffraction analysis

The XRD diffractograms of raw, digested, and bleached harakeke fibre were obtained using an EMPYREAN diffractometer system (PANalytical). The fibres were chopped and pressed into a disk, using a cylindrical steel mould. Then, analysis was performed over a range of 5−65° at a scanning speed of 1° min^{-1} with a scan step of 0.02° using a CuKα radiation (λ=1.54 nm) The cellulose crystallinity index (*CrI %*) of the fibres was calculated following the Segal method, using equation 2.

$$CrI\% = \frac{I_{002} - I_{am}}{I_{002}} \text{ x } 100 \qquad (2)$$

where, I_{002} is the maximum intensity of the (002) lattice diffraction peak of cellulose and I_{am} is the intensity of diffraction of the amorphous component.

2.2.7. Mechanical testing

The tensile test specimens for PLA and the composites were prepared according to EN ISO 527, while flexural test specimens were prepared according to EN ISO 178. These tests were conducted on an Instron® 5982 universal testing machine equipped with a 5 kN load cell, running at a crosshead speed of 5 mm min^{-1}, and 10 mm min^{-1} for tensile and flexural tests, respectively. During tensile testing, the strain was measured using a 25 mm extensometer fixed at the middle of the specimen. Prior to mechanical testing, the test specimens were preconditioned in a climate chamber at 23 °C and 50% relative humidity for 48 h. Five specimens were tested during tensile and flexural tests and average results were recorded for the tensile strength (TS), tensile modulus (TM), flexural strength (FS) and flexural modulus (FM).

2.2.8. Thermogravimetric and differential scanning calorimetric analysis

Thermogravimetric analysis (TGA) was performed using a Perkin Elmer STA 8000 thermal analyzer. The sample, weighing about 10-20 mg was placed in a crucible and analysis was performed under argon atmosphere at a gas flow rate of 40 mL min^{-1} while being heated at 10 °C/min from 30 °C to 600 °C.

Differential scanning calorimetry analysis (DSC) of PLA and the composites was performed using a TA instrument (Netzsch DSC 3500 Sirius). Samples were heated from 20 to 200 °C at 10 °C/min under a nitrogen flow using a gas flow rate of 60 mL/min. From the DSC thermogram, the glass transition temperature (T_g), crystallization temperature (T_c) and melting temperature (T_m) were determined. In addition, the crystallinity (I_{DSC}) of PLA in the composite was calculated from the heat of fusion of the tested sample and a reference sample (PLA)with 100% crystallinity, using equation 3.

$$\%crystallinity\ (I_{DSC}) = \frac{\Delta H}{\Delta H_m W}\ x\ 100\% \quad (3)$$

where, ΔH and ΔH_m represents the heat of fusion of the samples, and a reference PLA with 100% crystallinity, respectively, while W is the mass fraction of the matrix. The crystallinity of PLA in the composites was calculated by using 93.6 J/g as the heat of fusion (ΔH_m) of reference PLA with 100% crystallinity [30].

2.2.9. Dynamic mechanical analysis

The dynamic mechanical analysis (DMA) was performed on a Perkin Elmer DMA800 Dynamic Mechanical Analyzer. A single cantilever mode was used to test the specimens (30 mm x 5 mm x 1.5 mm) by heating the specimens at a rate of 2 °C/min from 23 °C to 140 °C. The displacement amplitude was 20 µm and the test was performed at a frequency of 1 Hz.

3. Results and discussion

3.1 Composition and properties of harakeke fibre

3.1.1 Composition of raw, digested, and bleached harakeke fibre

The lignin and carbohydrate content of the fibres are presented in Table 1. It is evident from the table that the raw fibre has higher lignin and hemicellulose content than the treated fibres. In contrast, the cellulose content is higher in the treated fibres than in the raw fibre. The cellulose content in the raw fibre was 46% and this increased to 77% in the digested, and 83% for the bleached fibre. The higher cellulose content in the treated fibres can be attributed to the removal of non-cellulosic components from the fibre, which served to increase the amount of cellulose per unit mass of the fibre. Removal of lignin and other non-cellulosic components from natural fibres can help to improve the crystalline nature of the fibre. This will in turn improve the fibre strength, and the strength of its reinforced composites due to increased reinforcing ability, and effective stress transfer within the composite. This is further discussed in subsequent sections.

Table 1 Chemical composition, and XRD parameters of the crystalline phase of raw, digested, and bleached harakeke fibre

	Composition (wt.%)		
Fibre type	Cellulose	Hemicellulose	Lignin
Raw fibre	46.00	18.80	15.84
Digested fibre	77.30	13.30	3.37
Bleached fibre	82.55	12.80	2.73

XRD Properties

Parameters	Raw fibre	Digested fibre	Bleached fibre
Peak position (°)	22.24	22.45	22.66
FWHM	3.13	1.81	1.79
d (Å)	3.99	3.95	3.92
Crystallite size (nm)	21.71	37.20	36.83
Crystallinity Index (%)	72.79	79.75	81.50

* Raw fibre refers to the as-received harakeke fibre
* Digested fibre is the fibre harakeke fibre treated with 5% NaOH and 2% Na_2SO_3
* Bleached fibre refers to the harakeke fibre digested with 5% NaOH and 2% Na_2SO_3, and then bleached with 5% H_2O_2 and 2.5% Na_2SiO_3

3.1.2 X-ray diffraction (XRD) properties of harakeke fibre

The XRD traces of raw, digested, and bleached harakeke fibre are illustrated in Figure 1. The two conspicuous peaks in the XRD curves of the fibres around $2\theta \approx 22°$ and $2\theta \approx 16°$ represent the crystalline and amorphous components of cellulose, respectively [31]. The crystallinity index calculated from these peaks are included in Table 1. The crystallographic (002) plane of cellulose in the raw, digested, and bleached fibre appeared at 2θ positions of 22.24°, 22.45°, and 22.66°, respectively.

The slight shift in the 2θ position of the fibre after digestion, and further shift after bleaching suggests a decrease in the interplanar spacing of the (002) planes in the digested and bleached fibre, compared to the raw fibre. This is an indication of closer packing of cellulose crystals in the digested and bleached fibre, due to the removal of lignin, hemicellulose, and other non-cellulosic components from the fibre after treatment [32]. Hence, the lower FWHM values of the digested and bleached fibres could be due to formation of hydrogen bonds between the cellulose chains freed by the removal of binding structures like hemicellulose and lignin, which resulted in rearrangement and closer packing [33]. This is confirmed by the higher cellulose crystal size and crystallinity of the digested and bleached fibres, which is believed to be due to higher cellulose content as seen in Table 1. Lower FWHM values could also be due to the trans-crystallinity (crystal growth across or through individual crystals) induced in the cellulose structure, by the digestion and bleaching treatments. The crystallinity index values in Table 1 shows that the bleached fibre has a higher crystallinity index than the fibre subjected to digestion only. This indicates the presence of higher crystalline cellulose structure in the bleached fibre, and this aligns with the result obtained from the carbohydrate analysis (Table 1).

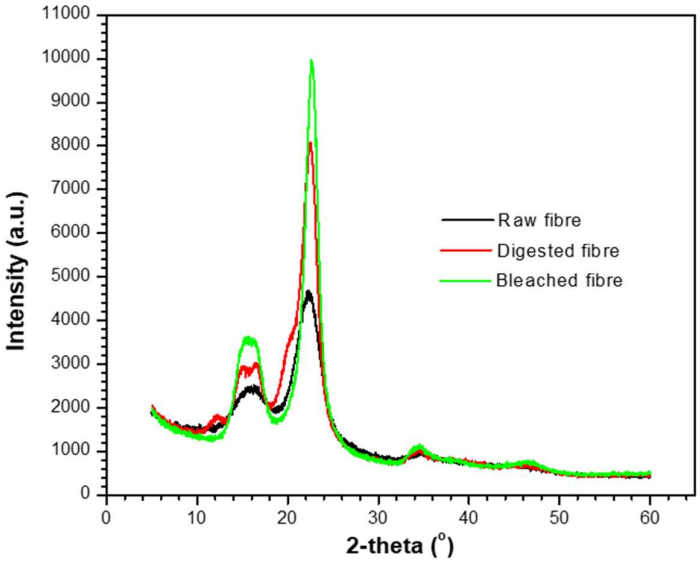

Figure 1 XRD traces of raw, digested, and bleached harakeke fibre

3.1.3 Morphological properties of raw, digested, and bleached harakeke fibre

The SEM images of raw, digested, and bleached harakeke fibre are shown in Figure 2. Surface of the raw fibre (Figure 2a) is smooth, likely due to the presence of cementing substances which tend to shield the fibre pores. These cementing substances can range from pectin, silica bodies, dirt particles and other soluble substances. In contrast, the surface of the digested fibre (Figure 2b) reveals rougher morphology which may be attributed to the removal of cementing substances from the fibre surface during digestion [34]. The alkali solution used for digestion helps to disrupt the bonding structure within the fibre, thereby removing the binding lignin and hemicellulose structures. This is responsible for the

roughness observed on the fibre surface (Figure 2b) and has been reported to facilitate mechanical interlocking between matrices and fillers during composite production [33, 35]. Therefore, this effect of fibre treatment on the strength of the resulting composite will be discussed in a later section.

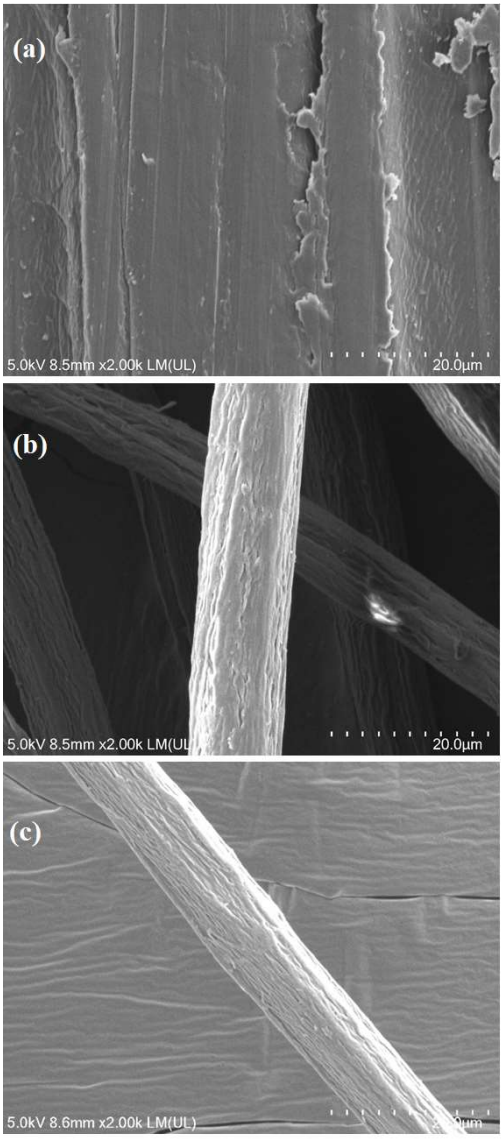

Figure 2 SEM images of (a) raw, (b) digested, and (c) bleached harakeke fibre

The SEM image of the bleached fibre (Figure 2c) reveals that the fibre is shrunken, with a rougher surface compared to Figure 2b. The bleaching treatment applied to the digested fibre helped to remove additional amounts of binding structure from the fibre, as presented in Table 1. This will invariably increase hydrogen bonding between the cellulose structures, due to removal of primary or secondary cell wall amorphous components [36, 37]. As the cellulose structure rearranges and packs more closely, the fibre shrinks, resulting in a reduced diameter, due to the increased fibrillation [33, 36]. The average diameters measured during SEM observation (result not shown) of the raw, digested, and bleached harakeke fibre were 495 µm, 11 µm, and 7 µm, respectively. The higher aspect ratio of the bleached fibre

can help to facilitate fibre distribution during composite fabrication, thereby resulting in higher reinforcing ability and increased composite strength [31, 38]. Likewise, the opening of pores on the fibre surface can help to improve fibre-matrix adhesion [8, 39]. These aspects of the modified fibres will be discussed further under the section on mechanical properties of composites. The removal of cementing and binding structures from the fibre through treatment, and formation of hydrogen bonds were verified through FTIR analysis which is discussed in the next section.

3.1.4 Fourier transform infrared spectroscopy (FTIR) of harakeke fibre

The FTIR spectra of raw, digested, and bleached harakeke fibres are illustrated in Figure 3. The notable peaks in the spectra of the raw fibre includes the −OH stretching vibration around 3200-3600 cm^{-1} [31]. The C−H stretching vibration of cellulose and hemicellulose is evident around 2850-2950 cm^{-1} [40], while the peak at 1737 cm^{-1} represents the C=O stretching peak of ester and carboxylic components of hemicellulose and lignin [31, 40]. The peak at 1647 cm^{-1} represents the =CH vibration of the aromatic skeletal in lignin [31], while the peak at 1422 cm^{-1} is attributed to the $-CH_3$ asymmetric, and C−H symmetric deformation. The peak at 1060 cm^{-1} represents the in-plane deformation of the easily cleavable C−O−C linkage in lignin [31].

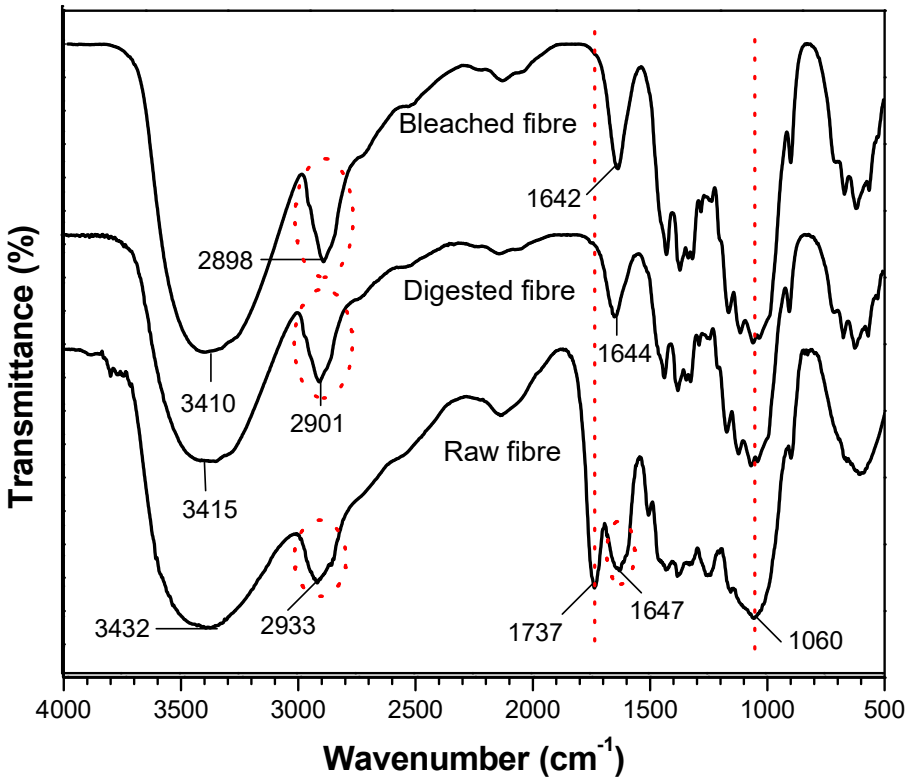

Figure 3 FTIR spectra of raw, digested, and bleached harakeke fibre

The −OH stretching vibration of bonded hydroxyl groups in the raw fibre shifted to a lower wavenumber in the digested and bleached fibre. This can be attributed to the structural changes caused the removal of lignin and hemicellulose through fibre treatment. This is believed to have influenced the reduced diameter of the treated fibre as discussed in

section 3.1.3. It should be noted that the downward shift is further in the bleached fibre, compared to the digested fibre probably because more binding structures were removed with bleaching, than was removed with digestion alone as reported in Table 1.

Another significant difference in the spectra of raw harakeke fibre and the treated fibres is the total disappearance of the C=O stretching peak at 1737 cm^{-1}. The absence of this peak in the spectra of the treated fibres confirm the dissolution of hemicellulose, and significant removal of lignin from the fibre during treatment [33, 40]. This explains the increased surface roughness of the digested and bleached fibres as shown in Figures 2b and 2c. There is a downward shift in the stretching vibration of C−H in cellulose and hemicellulose from 2933 cm^{-1} in the raw fibre, to 2901 cm^{-1} in the digested fibre, and 2898 cm^{-1} in the bleached fibre. This is attributed to the removal of hemicellulose, and repacking of the cellulose structure. Furthermore, removal of binding structure, namely lignin from the treated fibres was confirmed by the downward shift of the vibrational frequency from the =CH groups in the aromatic skeletal (methyl, methylene and methoxy groups) of lignin around 1647 cm^{-1}. The downward shift of this peak is an indication of structural deformation of lignin [41], which was further confirmed by the split in the aromatic C−H in-plane deformation peak at 1060 cm^{-1}. This FTIR result supports the SEM observation, and the carbohydrate analysis.

3.1.5 Thermal properties of harakeke fibre

The TGA curves of raw and treated fibres are illustrated in Figure 4a. As seen in the figure, there is a general drop in weight of all the fibre types in the temperature range from room temperature to around 130 °C due to the release of preabsorbed moisture [39]. Degradation in natural fibres generally starts at the amorphous regions, followed by the crystalline regions. The degradation of lignin starts around 160 °C, hemicellulose degradation starts around 220 °C, while cellulose degradation commences around 315 °C [39]. Although crystalline cellulose has higher degradation temperature, it has been revealed by literature that portions of the lignin component would normally degrade at higher temperature, in the range, and above the degradation temperature of crystalline cellulose [7, 42], due to the complex structure of lignin. Therefore, the early degradation observed in the raw fibre as seen in Figure 4a can be attributed to the degradation of amorphous non-cellulosic components such as lignin and hemicellulose. Due to the significant removal of non-cellulose components from the treated fibres, the thermal degradation in the treated fibres is mainly dependent on the crystalline cellulose. This is responsible for the higher thermal stability of the treated fibres

The thermal degradation temperature (T_d) of the fibres was derived from the DTG curve in Figure 4b. The thermal properties of the fibres, including onset temperature of thermal degradation (T_{onset}), and maximum thermal decomposition temperature (T_d) are presented in Table 2. In addition, the amounts of residue recorded at 600 °C are included in Table 2. The amount of residue recorded for the fibre as seen in Table 2 can be associated with the proportion of non-cellulosic components in the fibre which would appear in the form of char or ash residue [41, 43]. The relative

lignin content of the fibres as discussed in section 3.1.1 and presented in Table 1 shows that the amount of lignin in the fibres is in the order of raw fibre > digested fibre > bleached fibre. Therefore, this is believed to have influenced the residue from the samples at 600 °C.

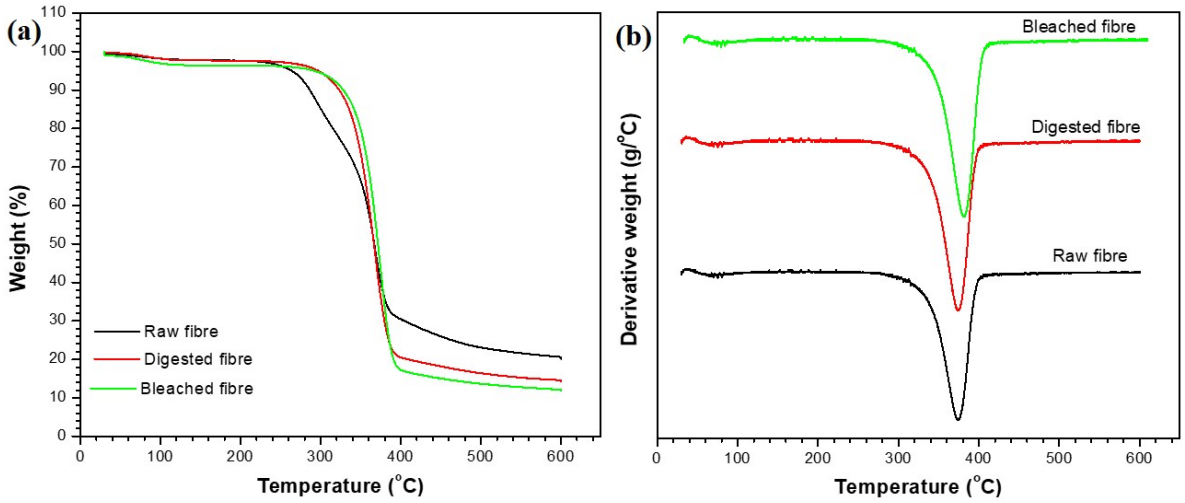

Figure 4 TGA curves of raw, digested, and bleached harakeke fibre

Table 2 Thermal properties of raw, digested, and bleached harakeke fibre

Samples	T_{onset} (°C)	T_d (°C)	Residual @ 600 (°C)	E_a (kJ/mol)
Raw Fibre	263.79	366.94	20.14	68.80
Digested Fibre	296.46	366.70	14.3	118.67
Bleached Fibre	291.29	371.50	11.80	125.61

Table 2 shows that the onset of thermal degradation is faster in the raw fibre compared to the treated fibre which is not unexpected. In the case of the treated fibres, the T_{onset} of the bleached fibre is lower than that of the digested fibre. As discussed in sections 3.1.2 and 3.1.4, bleaching of harakeke fibre facilitated increased formation of intermolecular hydrogen bonds between the cellulose molecules Therefore, the lower T_{onset} of the bleached fibre could be due to the large interface area created through bond formation. This might have permitted heat penetration at the unstable sites, particularly the amorphous regions of cellulose. Nevertheless, it is interesting that the T_d of the bleached fibre is higher than the digested fibre (see Figure 4 and Table 2). This indicates higher overall thermal stability of the bleached fibre, than the fibre digested alone. The reason for this might be due to the higher number of hydrogen bonds in the bleached fibre which restricted the continued ingress of heat. This will invariably shift the maximum decomposition temperature to the higher temperature range due to higher heat resistance of the more structured crystalline cellulose, as confirmed through XRD analysis and discussed in section 3.1.2.

In addition to its ability to help in determining the thermal degradation temperature (T_d), the DTG data can equally assist in calculating the activation energy associated with thermal degradation of natural fibres [33]. The activation energy (E_a) is a good indicator of the energy barrier that hinders molecular chain mobility in the fibre, which in turn retricts thermal degradation. Therefore, the thermal stability of the fibres was further investigated through kinetic study, using the TGA data according to the method described by Broido [44]. The kinetic parameter for thermal decomposition of the fibres was determined using equation 4 as follows:

$$ln\left(ln\frac{1}{y}\right) = -\frac{E_a}{RT} + ln\left(\frac{RZ}{E_a\beta}T_{max}^2\right) \quad (4)$$

where, y is the fraction of non-volatilized material as yet undecomposed, T_{max} is the temperature of the maximum reaction rate (°C), β is the heating rate (°C min^{-1}), Z is the frequency factor, E_a represents the activation energy (J mol^{-1}) and R is the gas constant (8.314 J mol^{-1} K^{-1}). The values of y can be obtained from the TGA data such that ln(ln(1/y)) can be calculated accordingly. By plotting a graph of 1/T (in Kelvin) on the x-axis and ln(ln (1/y)) on the y-axis, the activation energy (E_a) associated with thermal decomposition of the fibres can be determined from the slope of the graph [45]. The plot of 1/T vs ln(ln (1/y)) for the raw, digested and bleached harakeke fibre is presented in Figure S1 of the supplementary information section. The R^2 value of the plots for all the fibres are above 0.9 which indicates that the linearity of the graphs are in good agreement with the Broido equation, and the E_a values for thermal decomposition of the fibres are included in Table 2. As seen in Table 2, the E_a of the bleached fibre is higher than that of the raw and digested fibres. This confirms the higher thermal stability of the bleached fibre, and this aligns with the TGA result.

3.2 Properties of PLA/harakeke composites

3.2.1 Mechanical properties of PLA/harakeke composites

The mechanical properties of PLA and PLA/harakeke composites containing different wt.% (10-30 wt.%) of digested and bleached harakeke fibre are illustrated in Figure 5. It can be seen from Figure 5a that the tensile strength (TS) of the composites initially increased following the addition of fibre up to 20 wt.% fibre content. After this, the TS decreased when the fibre content was increased to 30 wt.%. On the other hand, the tensile modulus TM in Figure 5b reveals an increasing value with increasing fibre content. The initial increase in TS of the composites above the TS of neat PLA can be attributed to effective reinforcement and the transfer of stress from the PLA matrix to the reinforcing fibre. At 20 wt.% fibre, the TS is 73.06 MPa and 74.45 MPa for digested and bleached fibre composites, respectively compared to 62.85 MPa of neat PLA. Further increase in fibre content from 20 wt.% to 30 wt.% resulted in decline of TS. This observation agrees with what was reported in a similar study [16], which is believed to be due to less wetting of the fibre by the PLA matrix at this fibre content. Serizawa et al., investigated the effect of varying amounts of kenaf fibre on the properties of kenaf fibre reinforced PLA composite. They reported that the maximum flexural strength and modulus

was attained at 20 wt.% fibre content [17]. Likewise, Komal et al., reported 20 wt.% banana fibre as the optimum fibre content when they varied the fibre content from 10-30 wt.% in banana fibre reinforced PLA composites [18]. A drop in mechanical performance of composites beyond what is defined as an optimum fibre content is often due to poor wetting of the fibre. Poor wetting will normally lead to agglomeration of fibre within the composite due to unfavourable distribution, thereby leading to the creation of large voids within the composite. As a result of this, the transfer of stress from the matrix to the reinforcing fibre will not be effective, which leads to the observed decrease in TS of the composites at 30 wt.% fibre content.

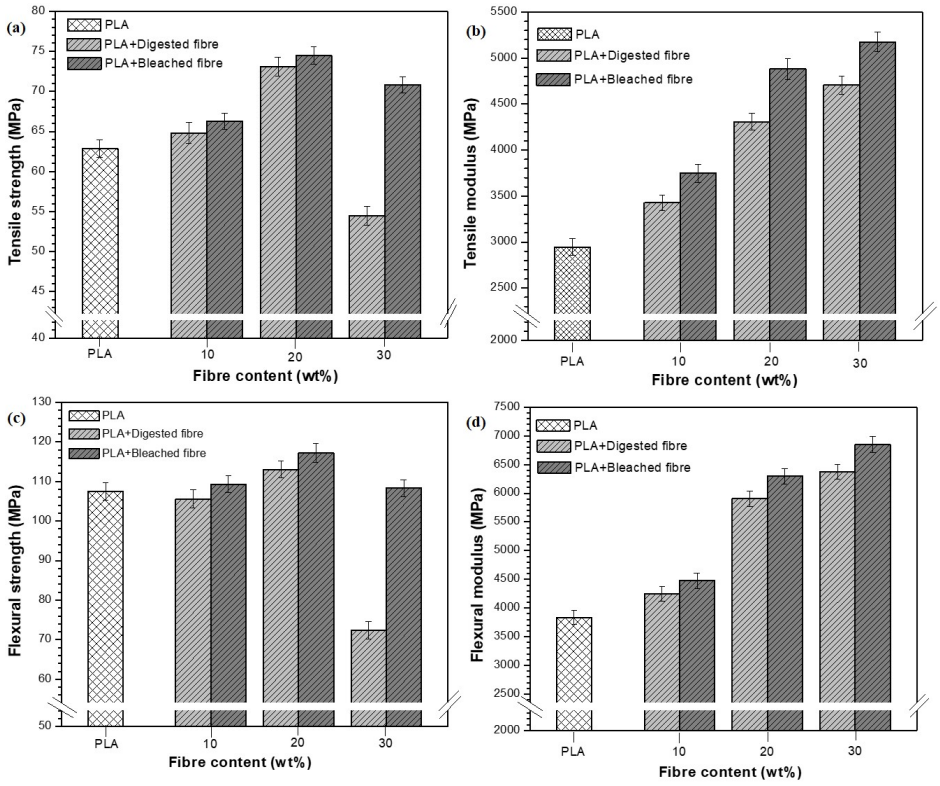

Figure 5 (a)Tensile strength, (b) tensile modulus, (c) flexural strength, and (d) flexural modulus of PLA and PLA/harakeke composites containing different wt.% of digested and bleached harakeke fibre

It is noteworthy that at the different fibre contents, the TS of bleached fibre composites is higher than the digested fibre. Literature revealed that the mechanical strength of natural fibre reinforced composites can be significantly influenced by the fibre diameter [5]. Specifically, large diameter fibres can trigger different local deformation processes within the composite including fibre pull-out, debonding of the fibre from the matrix, or fibre fracture. As discussed in section 3.1.3, the diameter of bleached harakeke fibre is smaller than that in digested fibre. Therefore, the wider diameter of the digested fibre might have contributed to the lower strength of the digested fibre composites, compared to the bleached fibre composites as seen in Figure 5a. In another vein, treatment of fibre through bleaching with peroxide has been reported to facilitate interfacial bonding between the fibre and polymer matrices, by acting as a coupling agent [10,

40]. This is believed to have contributed to the higher strength of the bleached fibre composites. Fibre pull-out, debonding of fibre from matrix, fibre fracture, and the extent of interfacial adhesion in the composites was assessed through SEM observation of the fractured surfaces of the composites which forms the subject of the next section.

Similar trends can be seen in the FS in Figure 5c and the TS in Figure 5a and the reason for this trend is as stated in the previous paragraph. In contrast to the trend observed for TS and FS, the tensile modulus (TM) and flexural modulus (FM) of the samples illustrated in Figure 5b (TM) and Figure 5d (FM) shows an increasing trend as fibre content was increased. This can be attributed to the high modulus of harakeke fibre, and this suggest that the strength and modulus of PLA/harakeke composites depend on different factors. Specifically, the strength is believed to be influenced by such factors such as wetting of fibre by the matrix, filler distribution, filler content, and fibre-matrix interfacial adhesion. In contrast, modulus of the composite seems to be more dependent on the filler content, and modulus of the fibre. Generally, in fibre reinforced polymer composites, there are always reports on the optimum fibre content for maximum strength. This is usually between 20-40 wt.% fibre content depending on the composite preparation method, type of filler, and matrix type. Some selected studies on natural fibre reinforced PLA composites are summarized in Table S1 in the supplementary information section. It is noteworthy that the TS and FS recorded at 20 wt.% fibre in this study is comparable to most of the previously published reports on reinforced PLA composites, even at higher fibre content values. This is a testament to the high reinforcing ability of harakeke fibre.

3.2.2 Morphological properties

The SEM images of the fractured surface (after tensile testing) of neat PLA, and PLA/harakeke composites containing 20 wt.% and 30 wt.% fibre are shown in Figure 6. It can be seen from Figure 6a, that the fractured surface of neat PLA is smooth, which is expected of brittle materials like PLA. For the composites with 20 wt.% fibre, it is evident that the length of pulled out fibre in the digested fibre (DF) reinforced composite, PLA+20 DF (Figure 6b) is longer than for those observed in composite reinforced with fibres subjected to bleaching (BF) (PLA+20 BF) (Figure 6c). The shorter pull-out fibres in Figure 6c indicates stronger interfacial adhesion between PLA and the bleached fibre [5, 46]. Likewise, strands, believed to be PLA can be seen on the surface of PLA+20 BF (Figure 6c). In relation to this, it was reported in the literature that treatment of natural fibre with peroxide imparts ester functionality on the fibre surface [40, 47]. Hence, the peroxide bleaching of harakeke fibre in the present study has likely imparted ester functionality on the surface that will make the fibre more compatible with PLA. Therefore, the polymer strands seen in Figure 6c are believed to be due to stronger interfacial adhesion resulting from mechanical bonding between the PLA and the bleached fibre. This, it is believed, has contributed to the higher mechanical strength of the bleached fibre composites as discussed in section 3.2.1.

The SEM images of the composites containing 30 wt.% fibre reveal a higher number of pull-out holes on the composite fractured surface. This suggests a reduced fibre-matrix interaction between PLA and harakeke at 30 wt.% fibre

content. When there is a higher percentage of fibre in the composite, this can result in poor wetting of the fibre by the matrix and would be responsible for the drop in mechanical strength of the composite at 30 wt.% fibre content, for both DF and BF as seen in Figures 5a and 5c. Although a drop in mechanical strength was recorded for both fibre types at 30 wt.%, it is noteworthy that the alignment and orientation of fibre in the PLA+30 DF composite is lesser than in the PLA+30 BF composites. This, in addition to poor fibre wetting is believed to have contributed to the higher drop in mechanical strength of the DF reinforced composite at 30 wt.% fibre content, compared to that of the BF reinforced composite.

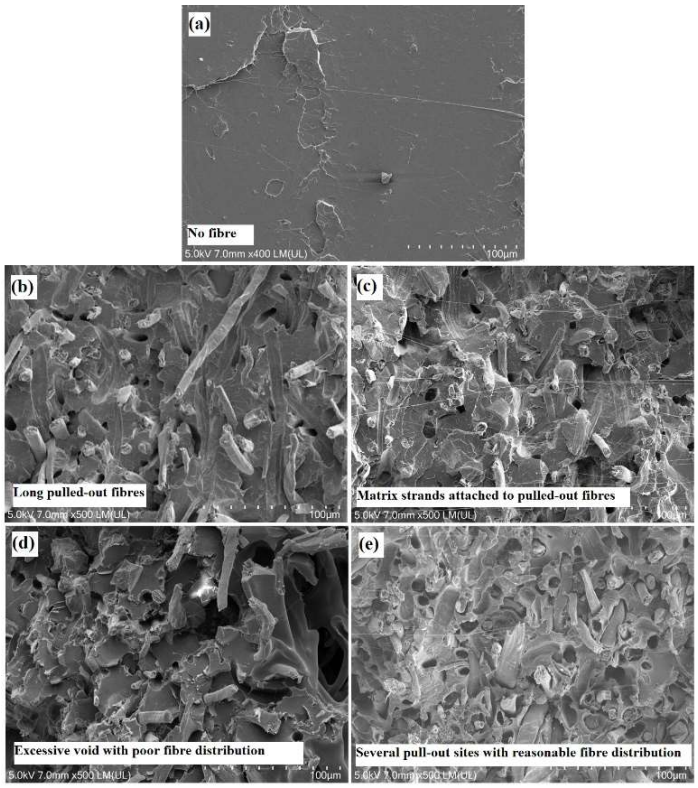

Figure 6 SEM images of (a) neat PLA, and PLA/harakeke composites containing (b) 20 wt.%F, (c) 20 wt.% BF, (d) 30 wt.% DF, and (e) 30 wt.% BF

3.2.3 Fourier transform infrared spectroscopy of composites

The bonding structures and extent of interfacial interaction between PLA and the treated harakeke fibres was further investigated through FTIR analysis. It should be noted that for ease of comparison, only the composites containing 20 wt.% fibre is discussed in this section. The FTIR spectra of PLA, PLA+20 DF, and PLA+20 BF are illustrated in Figure 7. The band in the FTIR spectra of PLA and the composites around 3200-3650 cm^{-1} is due to the stretching vibration of the−OH groups in cellulose, and the terminal hydroxyl groups in PLA [31], while the band around 2850–3050 cm^{-1} is attributed to symmetric and asymmetric stretching of C−H from methyl and methylene groups in cellulose. The peak at 1750 cm^{-1} is assigned to the C=O stretching vibration of acetyl and carboxylic acids moieties [31], and the ester components from PLA. The peak at 1455 cm^{-1} is a characteristic $-CH_3$ bending mode, whereas the peak at 1379 cm^{-1} is

attributed to C−H deformation [31]. In addition, stretching of the C–O group of carboxylic acid and the ester components of PLA is represented by the peak at 1091 cm^{-1}.

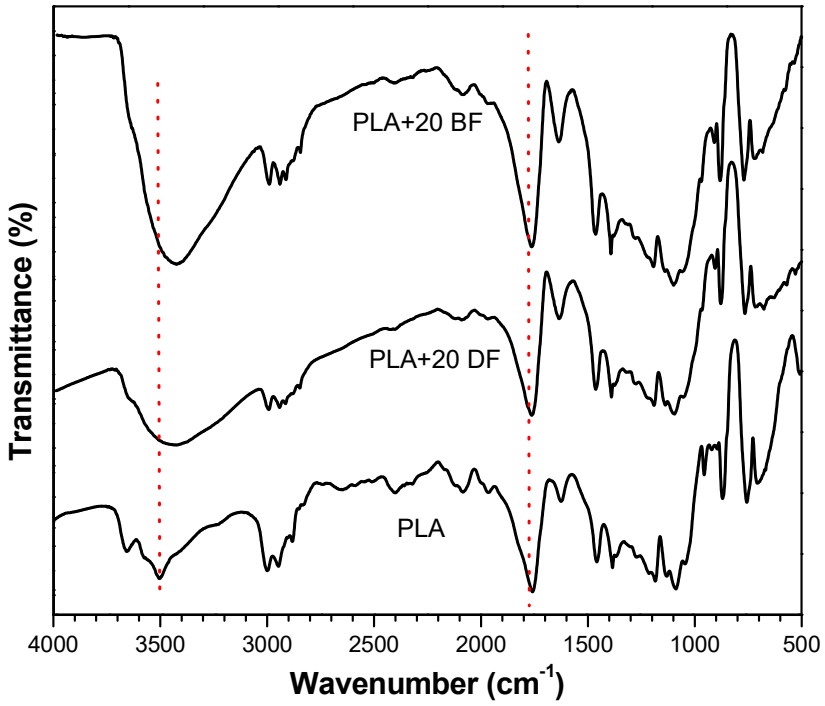

Figure 7 FTIR spectra of PLA, and PLA/harakeke composites containing different 20 wt.% of digested fibre (DF) and bleached harakeke fibre (BF)

It can be seen in Figure 7 that the −OH stretching vibration around 3200-3650 cm^{-1} in the spectra of PLA was widened in the spectra of the composites which suggests an increased intermolecular number of hydrogen bond due to increased number of −OH groups available for bond formation in the fibre cellulose, brought about by surface modification [31] This is supported by the slight movement of this peak to a lower wavenumber in the spectra of the composites, which is attributed to the formation of hydrogen bonds between the −OH of the fibres, and the terminal hydroxyl groups of PLA. In addition, the interaction between PLA and the fibres can be through bond formation between the cellulose −OH group of the fibres and C=O of PLA [48]. This is confirmed by the slight peak shift from 1750 cm^{-1} in the spectra of neat PLA, to a lower wavenumber value in spectra of the PLA/harakeke composites which indicates esterification reaction between the terminal −COOH groups of PLA and the −OH groups of harakeke fibre [48].

It is noteworthy that the downward shift of the band around 3200-3650 cm^{-1} and the peak at 1750 cm^{-1} is more significant than the shift observed in the spectra of the bleached fibre composite (PLA+20 BF), compared to the digested fibre composite (PLA+20 DF). This is an indication of a higher interaction between the bleached fibre and PLA, and this aligns with the SEM observations discussed earlier. The higher interaction between PLA and the bleached fibre as confirmed through this FTIR analysis is believed to have contributed to the higher mechanical properties of the bleached fibre composites as discussed in section 3.2.1.

3.2.4 Thermal properties of composites

The TGA curves of PLA and the composites are illustrated in Figure 8a. As seen in the figure, the TGA curves follow a similar trend. The onset of thermal degradation is above 300 °C and the drop in weight continued up to 400 °C. The onset of thermal degradation (T_{onset}) and the thermal degradation temperature T_d) of the samples are summarized in Table 3. In addition, the amount of residue remaining at T≥500 °C of the samples are included in Table 3. The T_{onset}, and T_d, of neat PLA is higher than that of the composites which is believed to be due to the intact structure of the PLA chains in neat PLA. The incorporation of fibres into PLA would distort the homogeneity of the PLA chain structure [16], which can in turn result in increased heat penetration sites as reported for micro crystalline cellulose (MCC) reinforced PLA composites [31]. It can also be due to the lower thermal stability of the fibre, compared to neat PLA [40]. From Figure 8a, and Table 3, it is evident that the bleached fibre composites are more thermally stable compared to the digested fibre composites, at all fibre contents.

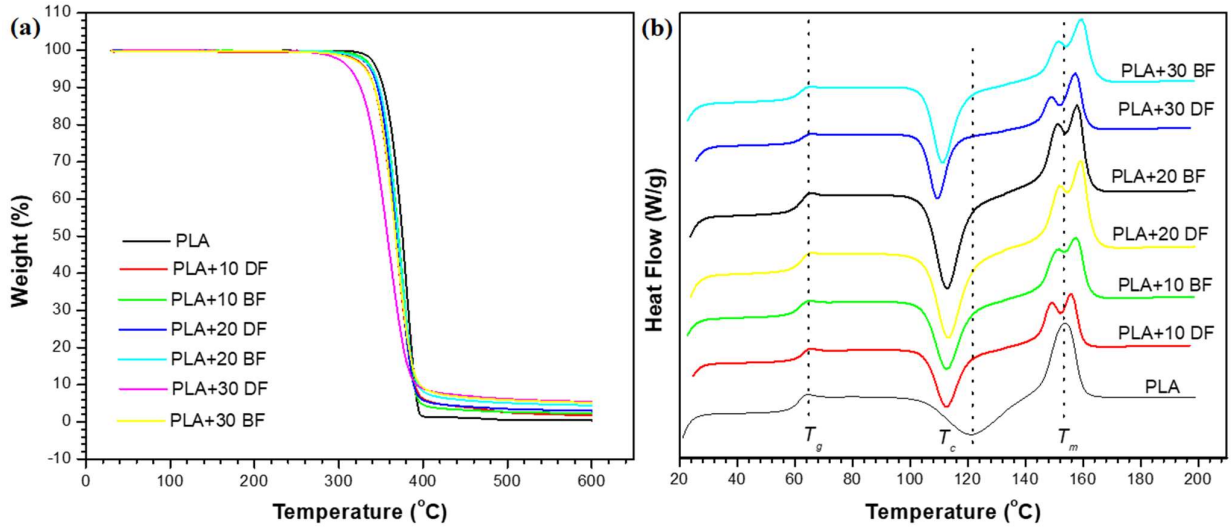

Figure 8 (a) TGA curves, and (b) DSC thermograms of PLA and PLA/harakeke composites containing different wt.% of digested fibre (DF) and bleached fibre (BF)

The DSC thermograms of PLA and the composites are shown in Figure 8b. From this figure it is possible to discern three successively distinct transitions which represent the glass transition temperature (T_g), crystallization temperature (T_c), and melting temperature (T_m). The DSC parameters of the samples were obtained from the thermograms, and the parameters are included in Table 3. It is evident in Figure 8b that the T_g of PLA was not significantly influenced by the inclusion of harakeke fibre. In contrast, the T_c of PLA in the composites can be seen to be notably influenced by the fibre. The addition of reinforcing fillers into semi crystalline polymers is known to result in an upward or downward shift in the T_c, and this often describes the ability of fillers to induce heterogeneous nucleation in the matrix [49]. The T_c of the samples presented in Figure 8b shows a downward shift in T_c of PLA in the composites. This is an indication of faster crystallization in the composites [50], which confirms the aforementioned heterogeneous nucleation activities on

the harakeke fibre. When cold crystallization occurs, it often results in the formation of imperfect crystals which can be verified through the melting peak of the sample [2].

The split in the melting peak (T_m) of the composites compared to neat PLA (Figure 8b) can be attributed to the formation of imperfect crystals in the composite due to the crystallization effects of the fibre on PLA. Usually, the imperfect crystals would melt at a lower temperature than the perfect crystals themselves. Hence, the double peaks observed around the T_m of PLA in the composites is because of perfect and imperfect crystals within the composite, due to the heterogeneous nucleation effects of the fibre. As seen in Figure 8b and presented in Table 3, the T_m of the composites is higher than that observed for neat PLA, most likely because the T_m of the composites was determined by the fusion of imperfect crystals formed during cold crystallization, and the fusion of spherulites formed during the process of recrystallization [2]. The effect of fibre treatment on the crystallization behaviour of PLA was further investigated through the calculation of the crystallinity index, using equation 3. The crystallinity index ($X_{DSC}\%$) of PLA and the composites are included in Table 3, which confirms the significant influence of fibre inclusion, on the crystallinity index of PLA. In addition, it was observed that at each fibre wt.% content, the bleached fibre composites exhibit a higher $X_{DSC}\%$ than the digested fibre composites. This indicates the formation of a larger number of crystallites within the bleached fibre composites and indicates that the bleached fibre did not only facilitate the formation of new crystals through heterogeneous nucleation but would also have led to the growth of existing spherulites. In another vein, the higher interfacial interaction between PLA and the bleached fibre as discussed in previous sections has favoured higher trans-crystallinity within the bleached fibre composite. Increased matrix crystallinity in known to support mechanical strength improvements in polymer composites. Therefore, the higher crystallinity of PLA in the bleached fibre composites than in the digested fibre composites has contributed to the superior mechanical strength of the bleached fibre composites as discussed in section 3.2.1.

Literature on this subject has revealed that one of the major factors influencing the thermal stability of composites, is the nature and strength of the fibre-matrix interfacial bonding [38]. Alkaline treatment of natural fibres increases the surface roughness of the fibres, thereby facilitating mechanical interlocking and interfacial adhesion between the fibre and matrix. In contrast, the dominant interfacial mechanism in peroxide treated fibres is chemical bonding [40]. The schematic illustration of the mechanism of reinforcement in digested and bleached harakeke fibre is shown in Figure 9. Results of the FTIR analysis and SEM observation discussed in previous sections suggests higher interaction between PLA and the bleached fibre, compared to the digested fibre. This can help to facilitate efficient distribution of thermal energy within the PLA/bleached fibre composite. The higher possibility for hydrogen bonding, and the increased distribution of fibre within the bleached fibre composites have both contributed to the higher thermal stability of the bleached fibre composites.

Table 3 Thermal properties of PLA and PLA/harakeke composites

TGA				DSC			
Sample code	T_{onset} (°C)	T_d (°C)	Residue (%) at T ≥ 500 °C	T_g (°C)	T_c (°C)	T_m (°C)	X_{DSC} (%)
PLA	345.25	375.48	0.58	61.90	121.00	154.00	26.53
PLA +10 DF	333.13	367.94	2.18	62.08	115.70	156.70	32.27
PLA +10 BF	339.60	370.18	2.67	62.13	116.70	157.49	33.93
PLA +20 DF	337.56	368.79	3.49	62.65	116.70	157.70	34.52
PLA +20 BF	338.75	370.87	5.06	63.22	116.30	158.70	36.13
PLA +30 DF	313.21	357.60	6.14	63.07	115.98	157.95	41.41
PLA +30 BF	331.15	367.25	6.90	63.15	116.85	158.97	41.49

3.2.5 Dynamic mechanical properties of PLA/harakeke composites

Dynamic mechanical analysis helps to determine the viscoelastic characteristics of polymer and polymer composites, and this is generally investigated through the storage modulus, loss modulus and the damping factor [7, 51]. The storage modulus (E′) curves of PLA and the composites are illustrated in Figure 10a. It can be seen in Figure 10a that the E′ of PLA and the composites dropped steadily around the glass transition region of PLA, which is attributed to increased PLA chain mobility. Increased chain mobility would result in softening and segmental movement of PLA molecules, and this would invariably produce a steep drop in E′ as seen in Figure 10a. The figure also shows that the E′ values of the composites are higher than in neat PLA which can be attributed to the stiffness imposed on PLA matrix by the reinforcing fibre. Increased stiffness would facilitate interfacial stress transfer within the composite [51].Therefore, this accounts for the higher modulus of the composites, compared to neat PLA. It is clearly seen in Figure 10a that the increase in fibre content produced increasing modulus values such that the E′ of the composites reach a maximum at 30 wt.% fibre. It is significant that the improvement in E′ of the composites when fibre content was raised from 20 wt.% to 30 wt.% is not as large as the improvement seen when raising the fibre content from 10 wt.% to 20 wt.%. This suggests that the reinforcement produced through good fibre distribution, and interfacial interaction within the composite was more effective at 20 wt.% fibre content than at 30 wt.%.

Literature has revealed that different factors can influence the E′ of composites, including matrix type, filler type, filler distribution, and filler-matrix interfacial adhesion [10, 38, 51]. Therefore, the higher E′ of the PLA-harakeke composites at 30 wt.% fibre content is not unexpected, considering the high modulus of harakeke fibre. It is interesting that at 20 wt.% fibre content, the bleached fibre composite (PLA+20 BF) exhibits a significantly higher E′ than in the digested fibre composite (PLA+20 DF). This can be associated with stronger interfacial bonding between PLA and the

bleached fibre as discussed in sections 3.2.2 and 3.2.3, in addition to the stiffness imposed on PLA by the fibre. The decomposition of organic peroxides leads to the formation of free radicals (RO˙) which are highly reactive. In the case of H_2O_2, OH radicals are produced and this highly reactive radical can react with the hydroxyl groups of the fibre thereby forming strong chemical bonds [40]. This will reduce the hydrophilic tendency of the fibre, thereby increasing its compatibility with PLA which favours fibre distribution in the matrix. Improved fibre distribution will facilitate effective stress transfer from PLA to the bleached fibre, which will in turn enhance the ability of PLA to withstand mechanical strain through recoverable viscoelastic distortion. This is believed to be responsible for the higher E′ of the bleached fibre composites above the digested fibre composites. To further assess the strength of the interface in the composites, the damping parameter (tan delta (δ)) was analysed.

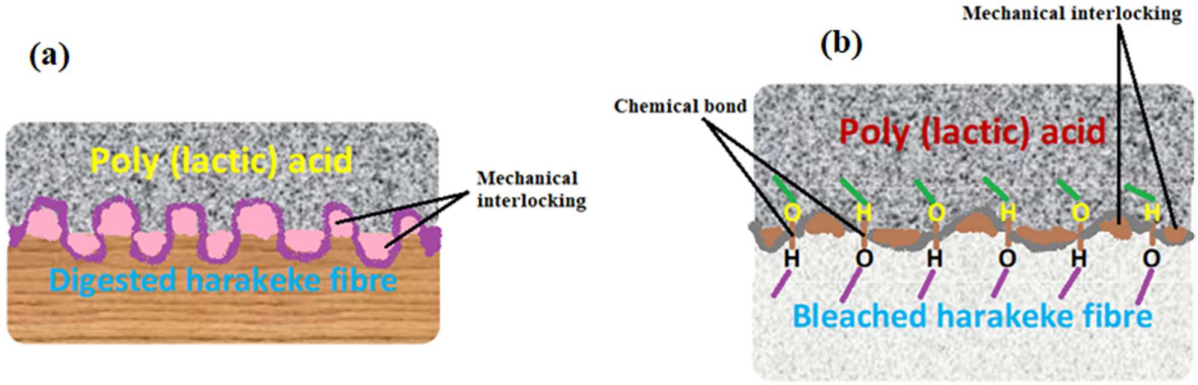

Figure 9 Illustration of the mechanism of PLA reinforcement by (a) digested, and (b) bleached harakeke fibre

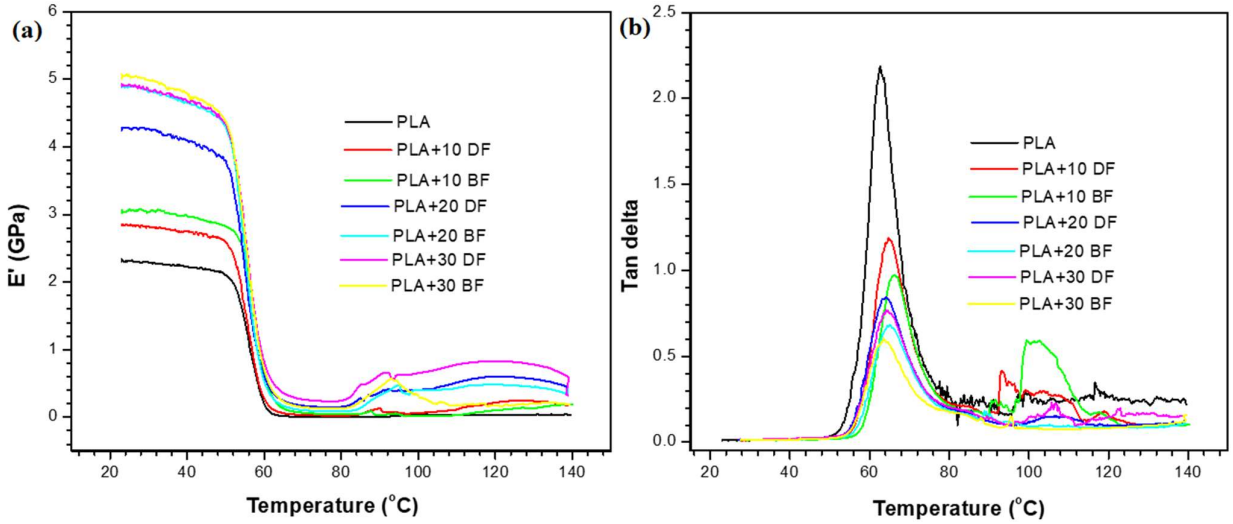

Figure 10 (a) Storage modulus, and (b) tan δ curves of PLA and PLA/harakeke composites containing different wt.% of digested and bleached harakeke fibre

The damping factor (tan δ) is the ratio of energy dissipated, to the energy stored when a material is subjected to dynamic constraints. The tan δ value is notable for its ability to accurately give an indication of the T_g of materials [51]. Usually, the T_g is obtained as the temperature at which the tan δ curve is at its maximum. The tan δ curves of PLA and the composites are illustrated in Figure 10b. The T_g obtained from the tan δ curves in Figure 10b and the maximum tan δ peak values are presented in Table 4. The T_g values obtained from the tan δ curves align with the DSC result which showed that the incorporation of harakeke only slightly affected the of T_g of PLA. The data in Table 4 show that the maximum tan δ peak of the composites is lower than observed for neat PLA. It can be seen in Figure 10b that the reduction in tan δ of the composites compared to PLA is quite large which indicates that the incorporation of harakeke fibre was more influential on the tan δ peak than on the T_g of PLA. Therefore, the tan δ peak was further analysed for the best mechanical performance composite in this study (i.e. 20 wt.% fibre content), to investigate the extent of interfacial adhesion in the composite. The tan δ peak was used to determine the adhesion factor A, and effectiveness coefficient C of PLA+20 DF and PLA+20 BF, in comparison with neat PLA.

Table 4 Effectiveness coefficient, adhesion factor, and tan δ parameter of PLA and PLA/harakeke composites containing 20 wt.% fibre

Sample code	Effectiveness coefficient (C)	Max tan δ peak value	Adhesion factor (A)	T_g (°C)
PLA	1.000	2.188	0.000	62.677
PLA +20 DF	0.071	0.841	-1.720	60.752
PLA +20 BF	0.053	0.681	-1.992	61.290

As reported in literature, the molecular mobility of polymer molecules around reinforcing fillers is often limited by strong interfacial adhesion between the matrix and the filler [51]. Hence, a strong interfacial adhesion would produce a low adhesion factor. The adhesion factor A of PLA and the composites was calculated using equation 5 as follows:

$$Adhesion\ factor\ (A) = \frac{1}{1-V_f}\frac{\tan\delta_c}{\tan\delta_p} - 1 \qquad (5)$$

where, tan δ_c and tan δ_p are the relative damping factors for the composite and neat polymer, respectively, whereas V_f is the fraction (by mass) of the filler. The relative damping of the materials is obtained at the glass transition temperature as indicated by the maximum in the tan δ peak [41]. The calculated A values are included in Table 4. It is evident that the bleached fibre composite has the lowest A value which serves as confirmation of stronger interfacial adhesion between the bleached fibre and PLA. This agrees with the FTIR results discussed in section 3.2.3 and this is believed to have

significantly contributed to the higher dynamic mechanical performance of the bleached fibre composite. The effectiveness of reinforcement, using bleached and digested fibre was also investigated by calculating the effectiveness coefficient. The effectiveness coefficient was obtained from the relationship between the ratio of the storage modulus E′ of the composite in the glassy and rubbery region, to that of the neat polymer. The effectiveness coefficient *C* was calculated using equation 6 as follows:

$$Effectiveness\ coefficient\ (C) = \frac{E_g'/E_r'\ (composite)}{E_g'/E_r'\ (resin)} \quad (6)$$

where, E'_g and E'_r represents the storage modulus in the glassy region and rubbery region, respectively. Generally, the reinforcing ability of the fibre is inversely proportional to the *C* value such that high reinforcing effectiveness will produce low *C* values. The calculated *C* value for PLA, and the composites are shown in Table 4 and the values confirms that the bleached fibre offers better reinforcing effectiveness to PLA than the digested fibre. This confirms the assumptions made based on the SEM observation of composites fractured surface (see Figure 6 and section 3.2.2), and it aligns with the results discussed in section 3.2.1.

4. Conclusion

Composites were prepared from PLA with different contents of digested and bleached harakeke fibre compounded through extrusion and injection moulded. Compared to digestion alone, combined digestion and bleaching treatment removed larger amount of non-cellulosic components from the fibre, which resulted in higher cellulose content. This increased the thermal stability of the fibre as confirmed through thermal analysis, which was attributed to the increased intermolecular cellulose hydrogen bonding in the digested and bleached fibre. Incorporation of the digested and bleached harakeke fibre into PLA produced higher mechanical and thermomechanical performance than the digested fibre alone. This was attributed to the effect of combined digestion and bleaching, which facilitated stronger interfacial interaction between PLA and the fibre, supported by the calculated adhesion factor and effectiveness coefficient. The mechanical test results showed that 20 wt.% fibre was the optimum fibre content and the composites strength recorded at this fibre content is comparable to what have been previously reported for higher fibre contents in some natural fibre reinforced composites. The result from this study shows that harakeke fibre is a promising reinforcement for PLA to produce high performance composites suitable for structural applications. In addition, combination of digestion and bleaching treatment could present added benefits for improving the reinforcing ability of natural fibres in polymer composites, through increased fibre distribution and stronger interfacial bonding. Based on this study, further research is recommended for increasing the filler content by exploring different coupling additives to extend the use of harakeke fibre reinforced composites in more diverse structural applications.

5. Acknowledgement

The authors acknowledge the funding from the New Zealand Ministry of Business, Innovation and Employment, under the Āmiomio Aotearoa project hosted by The University of Waikato (UOWX2004). The first author also appreciates the financial support through a Research & Enterprise Award (108023) provided by the University of Waikato.

References

[1] Scaffaro R, Lopresti F, Botta L. PLA based biocomposites reinforced with Posidonia oceanica leaves. Composites Part B: Engineering. 2018;139:1-11.

[2] Serra-Parareda F, Delgado-Aguilar M, Espinach FX, Mutjé P, Boufi S, Tarrés Q. Sustainable plastic composites by polylactic acid-starch blends and bleached kraft hardwood fibers. Composites Part B: Engineering. 2022:109901.

[3] Rangappa SM, Siengchin S, Dhakal HN. Green-composites: Ecofriendly and sustainability. Applied Science and Engineering Progress. 2020;13(3):183-4.

[4] Thyavihalli Girijappa YG, Mavinkere Rangappa S, Parameswaranpillai J, Siengchin S. Natural Fibers as Sustainable and Renewable Resource for Development of Eco-Friendly Composites: A Comprehensive Review. Frontiers in Materials. 2019;6.

[5] Bartos A, Nagy K, Anggono J, Purwaningsih H, Móczó J, Pukánszky B. Biobased PLA/sugarcane bagasse fiber composites: Effect of fiber characteristics and interfacial adhesion on properties. Composites Part A: Applied Science and Manufacturing. 2021;143:106273.

[6] Samouh Z, Molnar K, Boussu F, Cherkaoui O, El Moznine R. Mechanical and thermal characterization of sisal fiber reinforced polylactic acid composites. Polymers for Advanced Technologies. 2019;30(3):529-37.

[7] Rajeshkumar G, Seshadri SA, Devnani G, Sanjay M, Siengchin S, Maran JP, et al. Environment friendly, renewable and sustainable poly lactic acid (PLA) based natural fiber reinforced composites–A comprehensive review. Journal of Cleaner Production. 2021;310:127483.

[8] Mazzanti V, Pariante R, Bonanno A, de Ballesteros OR, Mollica F, Filippone G. Reinforcing mechanisms of natural fibers in green composites: Role of fibers morphology in a PLA/hemp model system. Composites Science and Technology. 2019;180:51-9.

[9] Yang X, Fan W, Ge S, Gao X, Wang S, Zhang Y, et al. Advanced textile technology for fabrication of ramie fiber PLA composites with enhanced mechanical properties. Industrial Crops and Products. 2021;162:113312.

[10] Getme AS, Patel B. A review: Bio-fiber's as reinforcement in composites of polylactic acid (PLA). Materials Today: Proceedings. 2020;26:2116-22.

[11] Ighalo JO, Adeyanju CA, Ogunniyi S, Adeniyi AG, Abdulkareem SA. An empirical review of the recent advances in treatment of natural fibers for reinforced plastic composites. Composite Interfaces. 2021;28(9):925-60.

[12] Pickering KL, Efendy MA, Le TM. A review of recent developments in natural fibre composites and their mechanical performance. Composites Part A: Applied Science and Manufacturing. 2016;83:98-112.

[13] Setswalo K, Oladijo O, Namoshe M, Akinlabi E, Sanjay M. The mechanical properties of alkali and laccase treated pterocarpus angolensis (mukwa)-polylactic acid (PLA) composites. International Journal of Biological Macromolecules. 2022;217:398-406.

[14] Tarrés Q, Melbø JK, Delgado-Aguilar M, Espinach F, Mutjé P, Chinga-Carrasco G. Micromechanics of Tensile Strength of Thermo-mechanical Pulp Reinforced Poly (lactic) Acid Biodegradable Composites. Journal of Natural Fibers. 2022:1-14.

[15] Siakeng R, Jawaid M, Asim M, Fouad H, Awad S, Saba N, et al. Flexural and Dynamic Mechanical Properties of Alkali-Treated Coir/Pineapple Leaf Fibres Reinforced Polylactic Acid Hybrid Biocomposites. Journal of Bionic Engineering. 2021;18(6):1430-8.

[16] Al Abdallah H, Abu-Jdayil B, Iqbal MZ. Improvement of mechanical properties and water resistance of bio-based thermal insulation material via silane treatment. Journal of Cleaner Production. 2022;346:131242.

[17] Serizawa S, Inoue K, Iji M. Kenaf-fiber-reinforced poly (lactic acid) used for electronic products. Journal of Applied Polymer Science. 2006;100(1):618-24.

[18] Komal UK, Lila MK, Singh I. PLA/banana fiber based sustainable biocomposites: a manufacturing perspective. Composites Part B: Engineering. 2020;180:107535.

[19] Sanjay MR, Madhu P, Jawaid M, Senthamaraikannan P, Senthil S, Pradeep S. Characterization and properties of natural fiber polymer composites: A comprehensive review. Journal of Cleaner Production. 2018;172:566-81.

[20] Akindoyo JO, Beg MDH, Ghazali S, Islam MR. The effects of wettability, shear strength, and Weibull characteristics of fiber-reinforced poly (lactic acid) composites. Journal of Polymer Engineering. 2016;36(5):489-97.

[21] Wehi PM, Clarkson BD. Biological flora of New Zealand 10. Phormium tenax, harakeke, New Zealand flax. New Zealand Journal of Botany. 2007;45(4):521-44.

[22] Le Guen MJ, Newman RH. Pulped Phormium tenax leaf fibres as reinforcement for epoxy composites. Composites Part A: Applied Science and Manufacturing. 2007;38(10):2109-15.

[23] Cruthers NM, Carr DJ, Laing RM, Niven BE. Structural differences among fibers from six cultivars of harakeke (Phormium tenax, New Zealand flax). Textile research journal. 2006;76(8):601-6.

[24] De Rosa I, Iannoni A, Kenny J, Puglia D, Santulli C, Sarasini F, et al. Poly (lactic acid)/Phormium tenax composites: Morphology and thermo-mechanical behavior. Polymer composites. 2011;32(9):1362-8.

[25] Newman RH, Le Guen MJ, Battley MA, Carpenter JE. Failure mechanisms in composites reinforced with unidirectional Phormium leaf fibre. Composites Part A: Applied Science and Manufacturing. 2010;41(3):353-9.

[26] Oksman K, Skrifvars M, Selin JF. Natural fibres as reinforcement in polylactic acid (PLA) composites. Composites Science and Technology. 2003;63(9):1317-24.

[27] Akindoyo JO, Beg MDH, Ghazali SB, Islam MR, Mamun AA. Preparation and characterization of poly (lactic acid)-based composites reinforced with poly dimethyl siloxane/ultrasound-treated oil palm empty fruit bunch. Polymer-Plastics Technology and Engineering. 2015;54(13):1321-33.

[28] Verma D, Goh KL. Effect of Mercerization/Alkali Surface Treatment of Natural Fibres and Their Utilization in Polymer Composites: Mechanical and Morphological Studies. Journal of Composites Science. 2021;5(7):175.

[29] Pettersen RC. Wood sugar analysis by anion chromatography. Journal of Wood Chemistry and Technology. 1991;11(4):495-501.

[30] Akindoyo JO, Beg MDH, Ghazali S, Heim HP, Feldmann M, Mariatti M. Simultaneous impact modified and chain extended glass fiber reinforced poly (lactic acid) composites: Mechanical, thermal, crystallization, and dynamic mechanical performance. Journal of Applied Polymer Science. 2021;138(5):49752.

[31] Bhiogade A, Kannan M, Devanathan S. Degradation kinetics study of Poly lactic acid (PLA) based biodegradable green composites. Materials Today: Proceedings. 2020;24:806-14.

[32] Sawpan MA, Pickering KL, Fernyhough A. Effect of various chemical treatments on the fibre structure and tensile properties of industrial hemp fibres. Composites Part A: Applied Science and Manufacturing. 2011;42(8):888-95.

[33] Kathirselvam M, Kumaravel A, Arthanarieswaran V, Saravanakumar S. Characterization of cellulose fibers in Thespesia populnea barks: Influence of alkali treatment. Carbohydrate polymers. 2019;217:178-89.

[34] Jaiswal D, Devnani G, Rajeshkumar G, Sanjay M, Siengchin S. Review on extraction, characterization, surface treatment and thermal degradation analysis of new cellulosic fibers as sustainable reinforcement in polymer composites. Current Research in Green and Sustainable Chemistry. 2022:100271.

[35] Tiwari YM, Sarangi SK. Characterization of raw and alkali treated cellulosic Grewia Flavescens natural fiber. International Journal of Biological Macromolecules. 2022.

[36] Duchemin B, Staiger MP. Treatment of Harakeke fiber for biocomposites. Journal of applied polymer science. 2009;112(5):2710-5.

[37] Ramlee NA, Jawaid M, Zainudin ES, Yamani SAK. Modification of oil palm empty fruit bunch and sugarcane bagasse biomass as potential reinforcement for composites panel and thermal insulation materials. Journal of Bionic Engineering. 2019;16(1):175-88.

[38] Rahman MZ. Mechanical and damping performances of flax fibre composites–A review. Composites Part C: Open Access. 2021;4:100081.

[39] Chougan M, Ghaffar SH, Al-Kheetan MJ, Gecevicius M. Wheat straw pre-treatments using eco-friendly strategies for enhancing the tensile properties of bio-based polylactic acid composites. Industrial Crops and Products. 2020;155:112836.

[40] Goriparthi BK, Suman K, Rao NM. Effect of fiber surface treatments on mechanical and abrasive wear performance of polylactide/jute composites. Composites Part A: Applied Science and Manufacturing. 2012;43(10):1800-8.

[41] Puglia D, Monti M, Santulli C, Sarasini F, De Rosa IM, Kenny JM. Effect of alkali and silane treatments on mechanical and thermal behavior of Phormium tenax fibers. Fibers and Polymers. 2013;14(3):423-7.

[42] Hong H, Xiao R, Guo Q, Liu H, Zhang H. Quantitively Characterizing the Chemical Composition of Tailored Bagasse Fiber and Its Effect on the Thermal and Mechanical Properties of Polylactic Acid-Based Composites. Polymers. 2019;11(10):1567.

[43] Qin L, Qiu J, Liu M, Ding S, Shao L, Lü S, et al. Mechanical and thermal properties of poly(lactic acid) composites with rice straw fiber modified by poly(butyl acrylate). Chemical Engineering Journal. 2011;166(2):772-8.

[44] Broido A. A simple, sensitive graphical method of treating thermogravimetric analysis data. Journal of Polymer Science Part A-2: Polymer Physics. 1969;7(10):1761-73.

[45] Oza S, Ning H, Ferguson I, Lu N. Effect of surface treatment on thermal stability of the hemp-PLA composites: Correlation of activation energy with thermal degradation. Composites Part B: Engineering. 2014;67:227-32.

[46] Georgiopoulos P, Kontou E, Georgousis G. Effect of silane treatment loading on the flexural properties of PLA/flax unidirectional composites. Composites Communications. 2018;10:6-10.

[47] Liu X, Dai G. Surface modification and micromechanical properties of jute fiber mat reinforced polypropylene composites. Express Polymer Letters. 2007;1(5):299-307.

[48] Sawpan MA, Pickering KL, Fernyhough A. Effect of fibre treatments on interfacial shear strength of hemp fibre reinforced polylactide and unsaturated polyester composites. Composites Part A: Applied Science and Manufacturing. 2011;42(9):1189-96.

[49] Akindoyo JO, Beg M, Ghazali S, Heim HP, Feldmann M, Mariatti M. Synergized high-load bearing bone replacement composite from poly (lactic acid) reinforced with hydroxyapatite/glass fiber hybrid filler—Mechanical and dynamic mechanical properties. Polymer Composites. 2021;42(1):57-69.

[50] Ruz-Cruz M, Herrera-Franco P, Flores-Johnson E, Moreno-Chulim M, Galera-Manzano L, Valadez-González A. Thermal and mechanical properties of PLA-based multiscale cellulosic biocomposites. Journal of Materials Research and Technology. 2022;18:485-95.

[51] Saba N, Jawaid M, Alothman OY, Paridah MT. A review on dynamic mechanical properties of natural fibre reinforced polymer composites. Construction and Building Materials. 2016;106:149-59.